Lactam Bridge Stabilization of α-Helices: The Role of Hydrophobicity in Controlling Dimeric versus Monomeric α-Helices†

Michael E. Houston, Jr., A. Patricia Campbell, Bruce Lix, Cyril M. Kay, Brian D. Sykes, and Robert S. Hodges*

Department of Biochemistry and Protein Engineering Network of Centres of Excellence, University of Alberta, Edmonton, Alberta, Canada T6G 2S2

Received November 20, 1995; Revised Manuscript Received May 29, 1996⊗

ABSTRACT: A series of lactam-bridged and linear 14 residue amphipathic α-helical peptides based on the sequence Ac-EXEALKKEXEALKK-amide were prepared in order to determine the effect of decreasing the hydrophobicity of the nonpolar face to helical content and stability. This was done by substituting position X by Ile, Val, and Ala. Lactam bridges spaced *i* to *i*+4 were formed between the side chains of Glu3 and Lys7 and Glu10 and Lys14 while the linear noncyclized peptides could potentially form *i* to *i*+4 salt bridges with the same residues. It was found that in all cases the lactam-bridged peptides were substantially more helical than the corresponding linear peptides as determined by CD spectroscopy. Moreover, the helical content approached 100% for the lactam-bridged peptides X = Ile and Ala and was greater than 80% for X = Val. For X = Ile and Val, this was partly due to the ability of the lactam bridges to enhance interchain interactions relative to the linear versions of the same sequence. Size-exclusion chromatography demonstrated that the Ile-based peptide associates as a dimer. The alanine-based lactam-bridged peptide was found to be monomeric as determined by concentration dependency studies and size-exclusion chromatography. Thermal denaturation studies in benign media indicated that the lactam-based peptides were very stable. The conformation of the Ala-based lactam peptide was further characterized by two-dimensional NMR spectroscopy and was found to be highly helical. The results demonstrate the ability of lactam bridges to stabilize the helical conformation and enhance dimerization of peptides based on a 3,4 hydrophobic heptad repeat. The substitution of Ala residues in the hydrophobic face of the α-helix can prevent dimerization and specify monomeric helical structure.

There is considerable interest in the design of short peptide segments that can adopt well-defined conformations in solution. Such peptides would be of considerable importance in the study of protein folding and receptor−ligand interactions and in the design of new medicinal agents. However, short peptides are generally assumed to populate multiple random-like structures. The observation that the N-terminal peptide fragments of ribonuclease A contained measurable secondary structure (Brown & Klee, 1971) initiated further studies into the factors important in stabilizing helices. The importance of charge−helix dipole interactions (Shoemaker et al., 1985; 1987) and intrachain side chain−side chain interactions in the stabilization of *de novo* designed α-helices has been reported (Marqusee & Baldwin, 1987; Scholtz & Baldwin, 1992; Zhou et al., 1993a). Other approaches using novel constructs have been used to stabilize α-helices. Kemp and co-workers (Kemp et al., 1991) designed a small organic template which served to nucleate helix formation by presenting hydrogen bond acceptors for the first three amide bonds of the peptide chain. Other methods have involved constraining the peptide backbone through covalent modification of specific side chains. For instance, Jackson et al. (1991) described the use of disulfide links between an enantiomeric pair of cysteine analogs spaced eight residues apart, which where capable of stabilizing the helical content of the peptide. Ghadiri and Choi (1990) have employed peptide−transition metal complexes to induce substantial helical character into an alanine-based peptide. Still others have cyclized the side chains of acidic (Asp, Glu) and basic amino acids (Lys, Orn) to induce helical content in peptides (Osapay & Taylor, 1990). Felix et al. (1988) and Madison et al. (1990) described the synthesis of human growth hormone releasing factor analogs in which lactams formed between aspartic acid and lysine residues increased the helical content of the peptide. This physical constraint not only increased the biologically active helical conformation of the peptide but also led to increased potency of the peptide.

Previously, we demonstrated the ability of Glu to Lys lactam bridges spaced *i*, *i*+4 residues apart to increase the helical content of synthetic amphipathic peptides (Houston et al., 1995). These peptides were based on the sequence Ac-EIEALKKEIEALKK-amide in which Ile and Leu are arranged in a 3,4 repeat typically found in coiled-coils. By incorporating two lactam bridges at the N- (Glu3−Lys7) and C-termini (Glu10−Lys14), the peptide adopted a highly helical conformation and was substantially more helical than its unconstrained counterpart of the same sequence. Of special interest was the dependency of the molar ellipticity at 222 nm on peptide concentration, suggesting that peptide−peptide association played a role in stabilizing the helical fold. In the present study, we wished to discern the oligomerization state of this peptide. In addition, we wish to determine the effect of hydrophobicity on the stability and oligomerization of the resulting lactam-bridged peptides by

† This research is an integral part of the Protein Engineering Network of Centres of Excellence supported by the Government of Canada.

* Author to whom correspondence should be addressed. Telephone: (403) 492-2758. Fax: (403) 492-1473. E-mail: robert.hodges@ualberta.ca.

⊗ Abstract published in *Advance ACS Abstracts,* July 15, 1996.

S0006-2960(95)02757-7 CCC: $12.00

progressively decreasing the hydrophobicity of the nonpolar face by amino acid substitutions. Through these manipulations, a switch from a very stable highly helical dimeric peptide to a very stable highly helical monomeric peptide was achieved as determined by circular dichroism (CD)[1] and SEC. The monomeric peptide was further characterized by 2D NMR, in order to verify the conformational constraints imposed by Glu-Lys *i* to *i*+4 lactam bridges.

MATERIALS AND METHODS

Peptide Synthesis and Purification. All peptides were prepared by solid-phase peptide synthesis using a benzhydrylamine hydrochloride resin on a Labortec SP 640 peptide synthesizer as described previously (Houston et al., 1995). The side chains of glutamic acid and lysine residues involved in lactam formation were protected as OFm and Fmoc derivatives, respectively. Lactam bridges were formed on the resin by deprotection of the desired side chains with 20% piperidine in NMP followed by cyclization with 5-fold excess of HBTU/HOBt/NMM in NMP with 5% HFIP (Houston et al., 1995). The peptides were cleaved from the resin by reaction with HF (10 mL/g of resin) containing 10% anisole for 1 h at −5 to 0 °C. The crude peptides were purified by reversed-phase high-performance liquid chromatography (RPC) on a SynChropak RP-4 preparative C4 column (250 × 21.2 mm internal diameter, 6.5 μm particle size, 300 Å pore size) (SynChrom, Lafayette, IN) with a linear AB gradient of 0.1% B/min with a flow rate of 5 mL/min, where solvent A is 0.05% trifluoroacetic acid in water and solvent B is 0.05% TFA in acetonitrile. The purity of the peptides was determined by reversed-phase HPLC The correct primary ion molecular weights of the peptides were confirmed by plasma desorption time of flight mass spectroscopy on a BioIon-20 mass spectrometer (Uppsala, Sweden). The peptides were further characterized by amino acid analysis. For amino acid analysis, peptides were hydrolyzed in 6 N HCl containing 0.1% phenol for 1 h at 160 °C in sealed evacuated tubes. The concentration of peptide solutions was deterrmined by amino acid analysis. Amino acid analysis was performed on a Beckman Model 6300 amino acid analyzer (Beckman, San Ramon, CA).

Size-Exclusion Chromatography. Size-exclusion chromatography was performed on a Pharmacia Superdex peptide HR 10/30 column (300 × 10 mm internal diameter, 13 μm particle size, fractionation range 100−7000 Da) (Pharmacia, Uppsala, Sweden) at a flow rate of 0.2 mL/min at room temperature. The eluent was a solvent of 50 mM KH_2PO_4, 100 mM KCl, pH 7.0. Stock solutions of the peptides were 3 mM. The concentration of eluted peptides was typically 30-fold lower (80−100 μM). The sequences of the size-exclusion standards were the following: (A) NH_2-FIPK-OH (504 Da); (B) NH_2-AGKDYDKIEE-OH (1168 Da); (C) NH_2-ATKKEVPLGVAADANKLG-OH (1783 Da); (D) Ac-EIEALKKEIGGLGGEIGALEKEIK-amide (2564 Da); and (E) NH_2-DTASDAAAAAALTAANAKAAAELTAANAA-AAAAATAR-amide (3236 Da).

CD Spectroscopy. Circular dichroism spectra were measured on a Jasco J-500C spectropolarimeter (Jasco, Easton, MD) equipped with a Jasco DP-500N data processor. A Lauda water bath (Model RMS, Brinkmann Instruments, Rexdale, Ontario) was used to control the temperature of the cell. Constant N_2 flushing was employed. The instrument was routinely calibrated with an aqueous solution of *d*-10-(+)-camphorsulfonic acid at 290 nm. Ellipticity is reported as mean residue molar ellipticity ([θ]), in degree centimeter squared per decimole, and calculated from the equation:

$$[\theta] = [\theta]_{obs}(\text{mrw})/10lc$$

where $[\theta]_{obs}$ is the ellipticity measured in degrees, mrw is the mean residue weight (molecular weight divided by the number of amino acid residues), *c* is the peptide concentration in grams per milliliter, and *l* is the optical path length of the cell in centimeters. CD spectra were the average of four scans obtained by collecting data at 0.1 nm intervals from 255 to 190 nm. Peptide concentrations were determined by amino acid analysis.

NMR Spectroscopy. ^{1}H NMR spectra for peptide 2EKA were acquired at 500 MHz using a Varian Unity 500 spectrometer. The hypercomplex method was used for acquisition of two-dimensional experiments (States et al., 1982) which typically incorporated 32 transients for each of 300 increments with 2048 data points along t_2, and included DQF COSY (Piatini et al., 1982; Rance et al., 1983), TOCSY (Bax & Davis, 1985), NOESY (Jeener et al., 1979; Macura & Ernst, 1980), JR-NOESY,[2] and ROESY (Kessler et al., 1987) spectra. Water suppression for all two-dimensional experiments except for the JR-NOESY experiment was achieved using presaturation for 2.0 s at a power level of 28 dB. Binomial water suppression was achieved for the JR-NOESY experiment using a jump-and-return read−pulse (Plateau & Guéron, 1982; Guéron et al., 1992). The TOCSY experiment employed a spin lock field of 7.12 kHz and was performed at 25.0 °C using a spectral width of 5400 Hz. The ROESY experiment employed a spin lock field of 4.51 kHz and was performed at 25.0 °C using a spectral width of 5400 Hz, and a mixing time of 150 ms. The DQF COSY experiments were performed at 5.0 °C using a spectral width of 6000 Hz. NOESY and JR-NOESY experiments were performed at both 5.0 °C and 25.0 °C using spectral widths of 6000 Hz, and mixing times of 150−500 ms to determine NOE buildup rates which were found to be linear up to 300 ms. The Fourier transformation of the spectra utilized sine bell processing with a phase shift of 90°, and zero-filling to 4K × 4K. Proton resonances were assigned at 5.0 and 25.0 °C (Table 3) using the sequential assignment technique (Wüthrich, 1986).

The JR-NOESY experiments were performed in addition to the NOESY experiments because the very rapid solvent exchange of the peptide backbone amide protons at higher temperatures necessitated a jump-and-return binomial water suppression in lieu of presaturation for suppression of the water signal. This fast exchange at 25.0 °C precluded the acquisition of a DQF COSY experiment at this temperature

[1] Abbreviations: HPLC, high-performance liquid chromatography; RPC, reversed-phase chromatography; SEC, size-exclusion chromatography; TFE, 2,2,2-trifluoroethanol; NMR, nuclear magnetic resonance; CD, circular dichroism; NOE, nuclear Overhauser effect; NOESY, two-dimensional nuclear Overhauser effect spectroscopy; JR-NOESY, jump-and-return two-dimensional nuclear Overhauser effect spectroscopy; ROESY, rotating-frame two-dimensional nuclear Overhauser effect spectroscopy; DQF COSY, two-dimensional double quantum filtered correlated spectroscopy; TOCSY, two-dimensional total correlation spectroscopy; ppm, parts per million; TFA, trifluoroacetic acid.

[2] Supplied by Varian Associates, 1991.

due to the low intensities of the backbone amide resonances. The ROESY experiment was performed at 25.0 °C since the faster correlation time of the peptide at higher temperatures caused the intensities of the NOE cross-peaks in the NOESY and JR-NOESY experiments to virtually disappear.

Temperature Coefficients and Coupling Constants. Temperature coefficients ($-\Delta\delta/\Delta T$ ppb) were obtained using data from JR-NOESY spectra acquired at 5.0 and 25.0 °C and from 1-D spectra acquired at 5.0, 10.0, 15.0, 20.0, and 25.0 °C, and were calculated from plots of chemical shift versus temperature which were linear for all amide protons in peptide 2EKA. $^3J_{NH\alpha CH}$ coupling constants for the peptide at 5.0 °C were obtained from 2K × 2K ($f_2 \times f_1$) DQF COSY spectra acquired at 5.0 °C. The spectra were zero-filled to 16K in the f_2 dimension and processed using 90° shifted sine bell weighting in the f_1 dimension and no weighting in the f_2 dimension. Traces for resolved cross-peaks were taken in ω_2 and then curve-fitted using a program written by R. Boyko and F. Sönnichsen (University of Alberta) which utilizes an iterative fitting procedure.

RESULTS

Experimental Design. The design of the peptides is based on the amphipathic lactam-bridged peptides reported by Houston et al. (1995). All peptides are 14 residues in length and based on the sequence Ac-EXEALKKEXEALKK-amide. Peptides with two lactam bridges are designated by the number 2 followed by the three letters EKX where EK represents the directionality of the lactam bridge (or salt bridge) from Glu to Lys (N-terminal to C-terminal direction) and X is either Ile, Val, or Ala. Noncyclized peptides are denoted as linear. This sequence allows for the formation of lactam bridges spaced *i* to *i*+4 apart between residues Glu3 and Lys7 and Glu10 and Lys14. In the case of the linear non-lactam-bridged peptides, the corresponding salt bridge can be formed (Marqusee & Baldwin, 1987). All peptides contain Glu at the N-terminus and Lys at the C-terminus to allow for favorable charged interactions with the helix dipole (Shoemaker et al., 1987). In addition, the N- and C-termini are capped in order to avoid any unfavorable helix−dipole interactions (Shoemaker et al., 1985, 1987).

Residues X and L are arranged in a 3,4 hydrophobic repeat involving positions *a* and *d* of the repeating heptad, denoted *abcdefg*, characteristic of a two-stranded α-helical coiled-coil. When X = Ile, the helical content of the lactam bridged peptide was dependent upon peptide concentration, suggesting that peptide oligomerization stabilizes the helical content significantly (Houston et al., 1995). In order to generate a highly helical monomeric peptide, we chose to substitute Ile at position *a* with the less hydrophobic amino acids Val and Ala. The *a* position was chosen because this position has been shown to be more promiscuous to amino acid replacements than the *d* position and β-branched amino acids at position *a* offer greater stability than at position *d* (Zhu et al., 1993). Through modulation of the hydrophobicity of the nonpolar face of the amphipathic α-helix, the tendency to dimerize should be diminished especially with the Ala substitutions where hydrophobicity is minimized and α-helical propensity is maximized (Zhou et al., 1994; Monera et al., 1995).

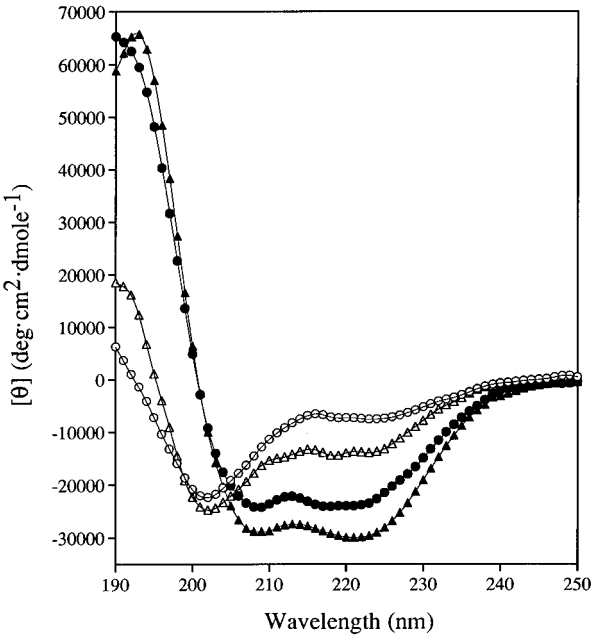

FIGURE 1: CD spectra at 20 °C in 50 mM KH_2PO_4, 100 mM KCl, pH 7.0, for peptides 2EKV linear (○), 2EKV (●), 2EKA linear (△), and 2EKA (▲).

CD Spectroscopy. The far-ultraviolet CD spectra of the lactam-bridged peptides and their linear counterparts are shown in Figure 1 and tabulated in Table 1. All spectra were measured at a peptide concentration of 750 μM under benign conditions (50 mM KH_2PO_4, 100 mM KCl, pH 7.0, 20 °C) in order to avoid any concentration dependency effects. The most noticeable feature of this figure is the high mean residue molar ellipticity exhibited by the lactam peptides relative to their linear homologs. All lactam-bridged peptides in this study have CD spectra indicative of an α-helix with minima at 221 and 208 nm. A maximum is

Table 1: Circular Dichroism Data of Lactam-Bridged and Linear Peptides: Peptides with Similar Sequences Are Grouped Together

peptide	$-[\theta]_{222}$ (deg·cm²/dmol)[a] benign	$-[\theta]_{222}$ (deg·cm²/dmol)[a] 50% TFE	$\Delta[\theta]_{222}$[b] (benign−TFE)	$\Delta[\theta]_{222}$[c] (linear−lactam) benign	helical content (%)[d] benign	helical content (%)[d] 50% TFE
2EKI linear[e]	18600	30000	11400		61	98
2EKI[e]	30350	32150	1800	11750	99	105
2EKV linear	7550	27500	19950		25	90
2EKV	24500	31100	6600	16950	80	101
2EKA linear	11450	28700	17200		37	93
2EKA	29900	31500	1600	18450	97	103

[a] Calculated molar ellipticity of the peptide at 222 nm. [b] $\Delta[\theta]_{222}$ is the difference between the ellipticity at 222 nm in benign buffer and in 50% TFE. [c] $\Delta[\theta]_{222}$ is the difference between the ellipticity at 222 nm of the linear peptide and lactam peptide of the same sequence. [d] The percent helical content was calculated from the ratio of the observed $[\theta]_{222}$ value divided by the predicted molar ellipticity. The predicted molar ellipticity (X^nH) was calculated from the equation $X^n\text{H} = X^\infty\text{H}(1 - k/n)$, using a $[\theta]_{222}$ value of −37 400 deg·cm²/dmol, for a helix of infinite length (X^∞H), *n* equal to 14, and *k* the wavelength-dependent constant equal to 2.50 (Chen et al., 1974) to give a value of −30 700 deg·cm²/dmol for 100% helical content. [e] Data taken from Houston et al. (1995).

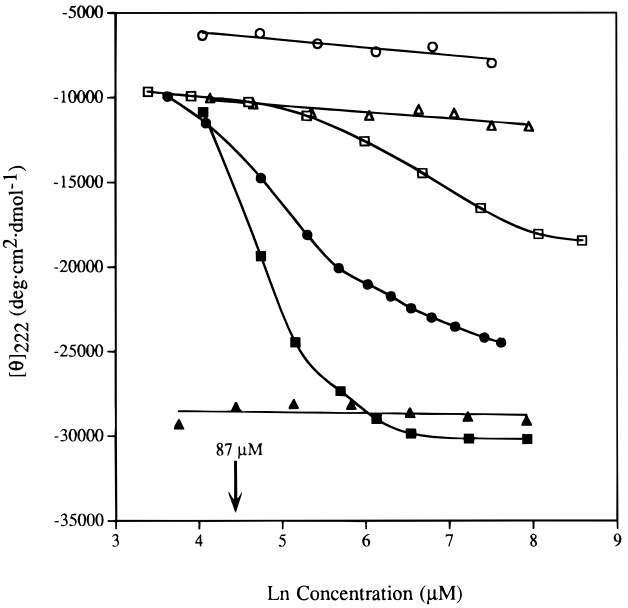

FIGURE 2: Concentration dependence of the mean residue molar ellipticity at 222 nm for peptides 2EKI linear (□), 2EKI (■), 2EKV linear (○), 2EKV (●), 2EKA linear (△), and 2EKA (▲). All measurements were performed in 50 mM KH_2PO_4, 100 mM KCl.

found at 192 nm for peptide 2EKA, while peptide 2EKV has a maximum at 190 nm. Peptide 2EKA has a molar ellipticity at 222 nm in benign medium of −29 900 deg·cm^2/dmol, which corresponds to 97% helical content. Peptide 2EKV contains less helical content (80%), and the maximum at 190 nm may be a result of a significant amount of random coil conformation populated by this peptide. The helical content is proportional to the mean residue molar ellipticity at 222 nm and was calculated according to Chen et al. (1974). In the presence of 50% TFE, an α-helix-enhancing solvent (Goodman & Listowsky, 1962; Goodman et al., 1971; Lehrman et al., 1990; Sönnichsen et al., 1992), small increases in helical content were observed for 2EKA and 2EKI while 2EKV showed a larger 21% increase in helical content (Table 1). The linear peptides exhibit considerably less helical content than the lactam-bridged peptides of the same sequence. The two linear peptides populate a significantly larger proportion of random coil as indicated by their minima at 201 nm. In the presence of 50% TFE, all linear peptides exhibit α-helical content of 90% or greater. The higher helical content for peptide 2EKA linear relative to 2EKV linear may simply reflect the higher helical propensity of Ala relative to Val ($\Delta\Delta G = -0.96$ and −0.42 kcal/mol, respectively; Zhou et al., 1994).

For peptide 2EKV, the plot of molar ellipticity at 222 nm versus concentration suggests that the helical content of the peptide is stabilized through peptide−peptide interchain interactions (Figure 2). However, at high peptide concentrations (>1.5 mM), the helical content does not approach a limiting value of ∼−31 000 deg·cm^2·dmol^{-1} as seen previously for peptide 2EKI (Houston et al., 1995). This suggests that interchain interactions are mediated through this nonpolar face of the 3,4 repeat. Moreover, this lack of a limiting mean residue molar ellipticity value at high peptide concentrations indicates that maximal helicity cannot be achieved because valine is not as effective as Ile in packing in the hydrophobic interface. This is consistent with previous experimental evidence which has suggested that hydrophobic packing and hydrophobicity within the interface are the major forces

Table 2: Size-Exclusion Chromatography Data of Lactam-Bridged and Linear Peptides

peptide	retention time (min)	experimentally determined MW[a]	calculated MW[b]
2EKA linear	57.91	1741	1599
2EKA	58.16	1715	1563
2EKV linear	57.09	1829	1655
2EKV	57.90	1802	1619
2EKI linear	57.34	1802	1683
2EKI monomer	56.90	1850	1647
2EKI dimer	49.90	2880	3294

[a] Experimentally determined molecular weights are derived from the equation of the linear fitting of the SEC standards. [b] Calculated molecular weights based on amino acid composition.

contributing to the overall stability of a coiled-coil (Hodges et al., 1990; Zhou et al., 1992a; Zhu et al., 1993). Decreasing the hydrophobicity further by substitution of Val by Ala maintains the high helical content similar to the Ile peptide; moreover, the helical content of the peptide remains constant over a range of 3000−40 μM. This behavior is typical of a monomeric helix and has been observed previously in alanine-based peptides stabilized by salt bridges (Marqusee et al., 1989). The high helical content is not seen in the 2EKA linear peptide which has the potential to form (i,i+3) or (i,i+4) salt bridges. Since 2EKA linear and 2EKA have the same sequence, the high helical content can be attributed to the 2 (i,i+4) lactams.

In order to determine the oligomerization states of the peptides, size-exclusion chromatography was performed. Figure 3 (top panel) illustrates the chromatogram of the five peptides used as molecular weight standards. All size-exclusion runs were performed in 50 mM KH_2PO_4, 100 mM KCl, pH 7.0, buffer. The molecular weights range from 504 for peptide A to 3236 for peptide E. A plot of log molecular weight versus retention time yields a straight line with a coefficient of linearity of 0.996 (Figure 3, middle panel). All the 14 residue peptides in this study, with the exception of peptide 2EKI, give rise to chromatograms with one peak and with retention times that are remarkably similar and vary by less than 1 min. The retention times, actual molecular weights, and molecular weights derived from the SEC standards are listed in Table 2. All experimentally determined molecular weights are clustered around 1750, which corresponds to a monomeric molecular weight, whereas the calculated molecular weights vary from 1563 to 1683.

For 2EKI, in addition to a peak at 57 min which corresponds to a monomeric molecular weight of 1850, a second smaller peak appears at 50 min which corresponds to a molecular weight of 2880 (Figure 3, bottom panel). The size of the dimer peak can be attributed to dilution that occurs upon injection of sample onto the column. While the stock solution of 2EKI was 2.80 mM, the concentration of the monomer peak was found to be 87 μM. At this concentration, the peptide is mostly unfolded as demonstrated previously (Houston et al., 1995). Dilution of the stock solution prior to loading onto the column resulted in diminution of the dimer peak (Figure 3, bottom panel insert). A complete loss of the dimer peak was observed after an 8-fold dilution of the 2EKI stock solution. This gives further proof that this peptide is in equilibrium between folded dimer and a monomeric species. These results correspond with the peptide concentration dependency study determined by CD (Figure 2) where at a peptide concentration of 87 μM 2EKI is mainly monomeric.

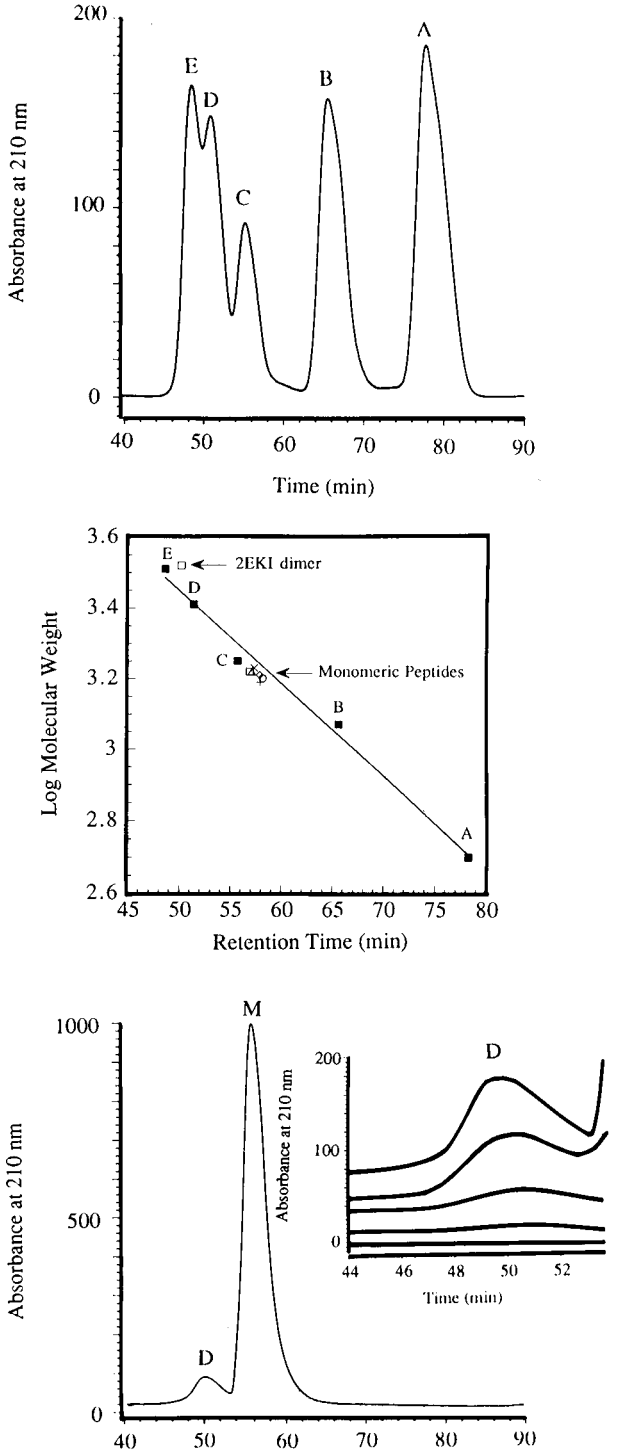

FIGURE 3: (Top panel) Elution profile of SEC standards. Molecular weights are (A) 504, (B) 1168, (C) 1783, (D) 2564, and (E) 3236. Sequences are listed under Materials and Methods. (Middle panel) Standard curve for the size-exclusion standards. Standards are indicated by (■). The letters A−E are as above. Lactam-bridged and linear peptides are denoted by 2EKA linear (+), 2EKA (○), 2EKV linear (△), 2EKV (◊), 2EKI linear (×), and 2EKI (□). Arrows indicate the position of the monomeric peptides and the 2EKI dimer. For the monomeric peptides, the experimentally determined molecular weights cluster around 1750. For the 2EKI dimer, the experimentally determined molecular weight is 2880 whereas the calculated molecular weight is 3294. (Bottom panel) Elution profile of 2EKI. Monomer is denoted as M and dimer as D. Insert: A blowup of the dimer peak indicating the loss of the dimer peak upon dilution (reading downward stock solution 2.80 mM, 3/4 dilution, 1/2, 1/4, and 1/8 dilutions of stock.

The thermal unfolding transition was found to be reversible for all lactam-bridged peptides, as indicated by the recovery

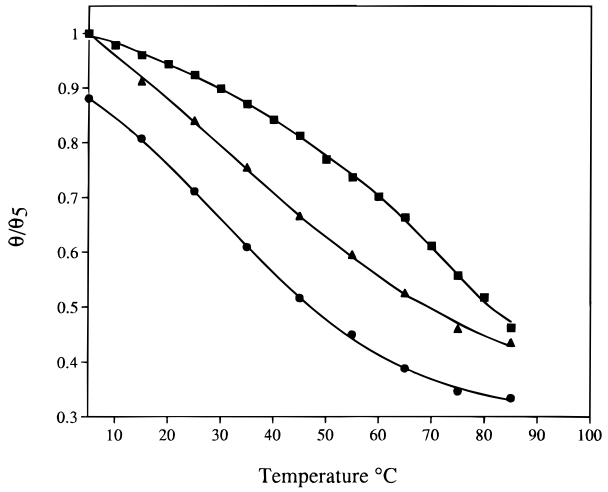

FIGURE 4: Thermal denaturations of 2EKI (■), 2EKV (●), and 2EKA (▲) in 50 mM KH_2PO_4, 100 mM KCl, pH 7.0. $[\theta]/[\theta]_5$ represents the ratio of the ellipticity at 222 nm at the indicated temperature to the ellipticity at 5 °C.

of the CD spectra upon cooling (data not shown). The thermal transitions of 2EKA, 2EKV, and 2EKI, at a concentration of 750 μM, are shown in Figure 4. The unfolding of the lactam-bridged peptides decreases with temperature in a manner analogous to the C peptide of ribonuclease and alanine-based peptides stabilized by salt bridges (Marqusee & Baldwin, 1987; Marqusee et al., 1989). The absence of a plateau at low temperature (5 °C) suggests that the transition to 100% helix formation is not fully complete. At high temperature, the spectra resemble the superposition of α-helix and random-coil conformations. For these peptides, the existence of an isodichroic point near 204 nm is consistent with each residue existing in either a helical or a random-coil conformation (data not shown) (Padmanabhan et al., 1990). The thermal transitions are very broad with a significant proportion of helix being present at 85 °C. We chose the $[\theta]_5$ value of 2EKI to represent the $[\theta]_{222}$ value of a maximally helical dimeric lactam bridged peptide. This value (−30 250 deg·cm^2/dmol) was used to calculate the fraction folded for 2EKV. For all peptides, a plot of fraction folded versus temperature reveals low cooperativity in the unfolding transitions which is in contrast to typical α-helices. This behavior has been seen in helical peptides constrained by *i* to *i*+7 disulfide bonds (Jackson et al., 1991) and template-nucleated α-helices (Kemp et al., 1991). This may simply be a result of residues constrained within the lactams retaining significant helical character while residues in the middle of the peptide are more free to relax to a random-coil conformation.

Resonance Assignments and Chemical Shifts. The ^{1}H NMR resonance assignments for 2EKA at pH 5.3, 5.0 and 25.0 °C, are presented in Table 3. An inspection of the αCH and NH proton shifts at both temperatures shows that they are upfield shifted, a phenomenon diagnostic of helical conformation. All 20 naturally occurring amino acids experience a mean α proton shift of −0.39 ppm (upfield from the random coil value) when placed in a helical configuration (Wishart et al., 1991). From Table 3, $\Delta\delta_{\alpha CH}$ values can be calculated for the αCH protons in 2EKA as the difference between the observed αCH chemical shift and the literature value of the αCH chemical shift for that residue in a random-coil conformation (Wishart et al., 1991). These values calculated at 5.0 and 25.0 °C are presented at the

Table 3: ^{1}H NMR Resonance Assignments of 2EKA

residue	NH	α-CH	β-H	γ -H	δ-H	ϵ-H and others
			(A) pH 5.3, 5 °C			
E_1	8.61	4.16	2.01, 2.08	2.30, 2.36		
A_2	8.57	4.12	1.46			
E_3	8.47	3.93	1.97, 2.39	2.61		
A_4	7.98	3.91	1.51			
L_5	8.02	4.13	1.56, 1.88	1.78	$(\delta CH_3)_2$ 0.89	
K_6	7.94	4.10	1.79	1.51	1.77	2.99, ϵNH 7.67
K_7	8.03	4.15	1.76	1.27, 1.47	1.95	2.72, 3.50, ϵNH 8.11
E_8	8.13	4.10	2.05, 2.14	2.25, 2.45		
A_9	8.10	4.17	1.52			
E_{10}	8.04	3.99	2.00, 2.50	2.40, 2.57		
A_{11}	7.99	3.90	1.50			
L_{12}	7.87	4.12	1.67, 1.78	1.72	$(\delta CH_3)_2$ 0.92	
K_{13}	7.75	4.08	1.69	1.49	1.77	2.99, ϵNH 7.67
K_{14}	7.55	4.02	1.68, 1.74	1.27, 1.47	1.94	2.77, 3.45, ϵNH 8.04
			(B) pH 5.3, 25 °C			
E_1	8.46	4.20	2.00, 2.06	2.34		
A_2	8.43	4.17	1.46			
E_3	8.36	3.92	2.01	2.39, 2.60		
A_4	8.01	3.92	1.50			
L_5	7.96	4.15	1.58, 1.85	1.76	$(\delta CH_3)_2$ 0.88, 0.92	
K_6	7.88	4.11	1.71, 1.85	1.47, 1.59	1.87	3.00, ϵNH * [2]
K_7	7.95	4.14	1.76	1.29, 1.49	1.79, 1.96	2.76, 3.49, ϵNH 7.93
E_8	8.06	4.12	2.14	2.30, 2.45		
A_9	8.02	4.16	1.51			
E_{10}	7.97	3.99	2.04	2.42, 2.57		
A_{11}	7.94	3.91	1.50			
L_{12}	7.81	4.14	1.65, 1.79	1.72	$(\delta CH_3)_2$ 0.90, 0.93	
K_{13}	7.71	4.13	1.72, 1.87	1.47, 1.59	1.71	3.00, ϵNH*
K_{14}	7.52	4.08	1.70	1.29, 1.49	1.94	2.82, 3.43, ϵNH 7.86

[a] The ϵNH protons of K_6 and K_{13} cannot be observed at 25 °C due to very rapid chemical exchange.

bottom of Figure 6. All αCH protons are upfield shifted at both temperatures, with the greatest upfield shifts (<-0.20 ppm) reserved for the trimer repeat E-A-L spanned by residues E3-A4-L5 and E10-A11-L12. This trimer repeat is located within the sequence encompassed by the two lactam bridges, and the substantial upfield shifts of the αCH protons in these E-A-L trimer repeats suggest that these are the regions most strongly constrained into a helical conformation by the presence of the lactam bridges. In contrast, the $\Delta\delta_{\alpha CH}$ values are somewhat less upfield shifted for residues situated on the N-terminal side of the bridges. For example, A9 has a $\Delta\delta_{\alpha CH}$ value close to zero. This could be indicative of some steric distortions in the helix imposed by the bridge, although the CD data are consistent with this peptide adopting a highly helical structure.

There is a striking similarity between the $\Delta\delta_{\alpha CH}$ values calculated for the peptide at 5.0 and 25.0 °C, suggesting that the conformation of the peptide is stable over this temperature range. The only difference observed between the values measured for the two temperatures is that the $\Delta\delta_{\alpha CH}$ values calculated at 25.0 °C for the N-terminal and C-terminal residues are slightly less negative than the same values calculated at 5.0 °C, suggesting that the peptide is fraying very slightly at the ends as the temperature is increased over the range of 20 °C.

NOESY Connectivities. NOE connectivities diagnostic of α-helix or 3_{10}-helix include a series of relatively strong $d_{NN}(i,i+1)$ connectivities, accompanied by medium-range $d_{NN}(i,i+2)$, $d_{\alpha N}(i,i+3)$, and $d_{\alpha\beta}(i,i+3)$ NOEs (Wüthrich et al., 1984; Wagner et al., 1986; Dyson & Wright, 1991). Figure 5 shows the d_{NN} and $d_{\alpha N}$ regions of the 500 MHz JR-NOESY spectrum of 2EKA at 5.0 °C with the important $d_{NN}(i,i+1)$, $d_{NN}(i,i+2)$, and $d_{\alpha N}(i,i+3)$ NOEs labeled (ROESY spectrum acquired at 25.0 °C not shown). Figure 6 is a schematic diagram showing the magnitude of the various NOE connectivities observed in JR-NOESY spectra of 2EKA at 5.0 °C and 300 ms and the ROESY spectrum at 25.0 °C and 150 ms. $d_{NN}(i,i+1)$, $d_{NN}(i,i+2)$, $d_{\alpha N}(i,i+3)$, and $d_{\alpha\beta}(i,i+3)$ NOE connectivities are observed from the N-terminus to the C-terminus of 2EKA and clearly demonstrate that the peptide is helical in conformation throughout its length. Evidence that 2EKA is helical from the very tip of the N-terminus to the very tail of the C-terminus is given by the presence of NOEs between the methyl group of the *N*-acetyl group to the backbone amide of E3, and by the presence of $d_{NN}(i,i+1)$ and $d_{NN}(i,i+2)$ NOEs between the C-terminal amino group to the backbone amides of K13 and K14. The analysis of NOESY spectra at 5.0 °C and ROESY spectra at 25.0 °C helped solve problems of backbone amide resonance overlap, and allowed assessment of the stability of the helix over the temperature range studied. Significantly, the same pattern of connectivities observed at 5.0 °C in the JR-NOESY is observed at 25.0 °C in the ROESY, which once again demonstrates that the helix is conformationally stable over the temperature range of 20 °C.

From the NOE patterns observed, it is difficult to discern between the formation of an α-helix versus a 3_{10}-helix. Generally, the 3_{10}-helix displays $d_{\alpha N}(i,i+2)$ NOEs, contacts which are not observed for the α-helix (Wagner et al., 1986). Weak $d_{\alpha N}(i,i+2)$ NOEs were observed as E10α/L12NH and A11α/K13NH NOEs connectivities (see Figures 5 and 6). This suggests that 2EKA may have some 3_{10} character at least at its C-terminus.

Further evidence for helicity, whether α or 3_{10}, comes from calculation of the ratio of the $d_{\alpha N}(i,i)$ and $d_{\alpha N}(i-1,i)$ NOEs, $d_{N\alpha}/d_{\alpha N}$, taken from the JR-NOESY experiment acquired at 5.0 °C and 300 ms. The magnitude of this ratio is dependent mainly on the ψ dihedral angle of residue $i-1$; thus, for $d_{N\alpha}$/

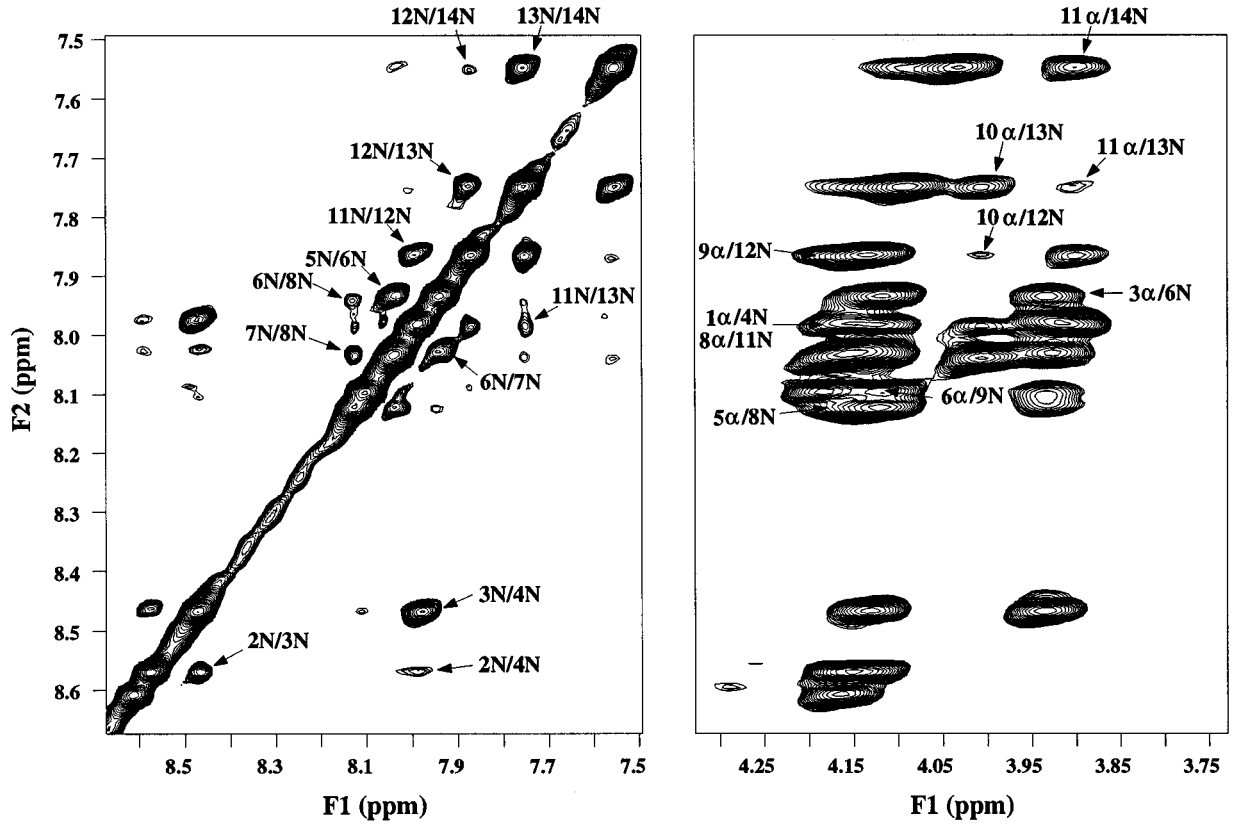

FIGURE 5: The d_{NN} and $d_{\alpha N}$ regions of the 500 MHz JR-NOESY spectrum of 2EKA. The peptide was in 90% H_2O/10% D_2O, pH 5.3 at 5.0 °C, whereas the mixing time of the experiment was 300 ms. $d_{NN}(i,i+1)$, $d_{NN}(i,i+2)$, and $d_{\alpha N}(i,i+3)$ connectivities which define helical conformation are labeled. $d_{\alpha N}(i,i+2)$ connectivities which suggest the presence of 3_{10}-helix are also labeled.

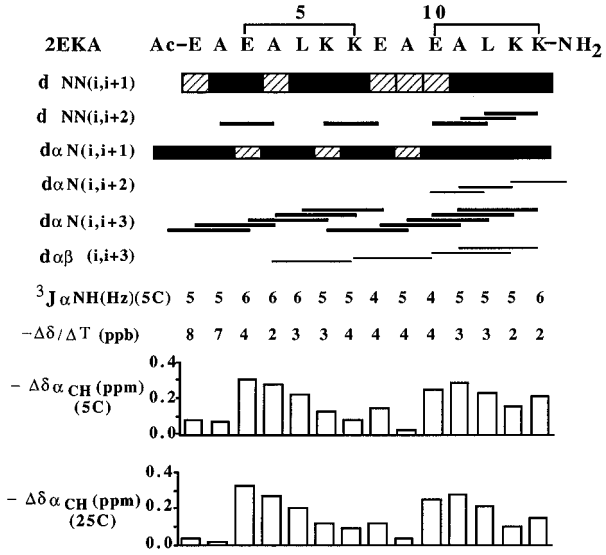

FIGURE 6: Schematic diagram showing the magnitude of various NOE connectivities observed in the NOESY (5 °C) and ROESY (25 °C) spectra of 2EKA. All connectivities represented in the figure were observed in both the NOESY and the ROESY spectra, except for A4α/K7NH, which could not be observed in the NOESY spectrum due to overlap. Hatched regions indicate connectivities which are probably present but which could not be assigned due to overlap. The figure also includes coupling constants ($^3J_{NH\alpha CH}$) measured at 5.0 °C, temperature coefficients ($-\Delta\delta/\Delta T$ ppb), and chemical shift ($\Delta\delta_{\alpha CH}$) information measured at 5.0 and 25.0 °C.

$d_{\alpha N} > 1.1$, $\psi(i-1)$ is in helical conformational space, whereas for $d_{N\alpha}/d_{\alpha N} < 0.83$, $\psi(i-1)$ is in extended conformational space (Gagné et al., 1994). Measurement of $d_{N\alpha}/d_{\alpha N}$ ratios for all possible residues in 2EKA yields values for $d_{N\alpha}/d_{\alpha N} > 1.1$, confirming that the peptide adopts a helical conformation.

Temperature Coefficients and Coupling Constants. The temperature coefficients and the coupling constants measured for 2EKA also strongly suggest helical conformation. Coupling constants measured for 2EKA at 5.0 °C show values of 4 Hz $\leq {}^3J_{NH\alpha CH} \leq$ 6 Hz, consistent with a ϕ angle in helical dihedral space ($\phi \leq -70°$) (Pardi et al., 1984). In general $^3J_{NH\alpha CH}$ values cannot be used to discern between the α helix and 3_{10}-helix, since $\phi = -57°$ for an α-helix, corresponding to $^3J_{NH\alpha CH} = 3.9$ Hz, and $\phi = -60°$ for a 3_{10}-helix, corresponding to $^3J_{NH\alpha CH} = 4.2$ Hz, values so close as to easily be within experimental error.

The temperature dependence of the amide proton chemical shift is an indication of possible intramolecular hydrogen bonding, and as such can be an indication of the formation of helix. For a random-coil peptide in water, the temperature coefficients of the amide proton resonances are expected to be $6 \leq -\Delta\delta/\Delta T \leq 10$ ppb, whereas for amides protected from exchange with the solvent these values are expected to decrease to $-\Delta\delta/\Delta T \leq 5$ ppb (Rose et al., 1985). The temperature coefficients for the amide backbone protons of 2EKA are shown in Figure 6. They show values of $-\Delta\delta/\Delta T \leq 4$ ppb for residues 3−14, consistent with the involvement of these amides in the O···NH($i,i+3$) hydrogen bonds present in the α-helix, or the O···NH($i,i+2$) hydrogen bonds present in the 3_{10}-helix. The backbone amides of residues E1 and A2 at the N-terminus of 2EKA show values of $-\Delta\delta/\Delta T \geq 7$ ppb, which suggests that these amides are not involved in hydrogen bonds. This is a reasonable result given that hydrogen bonding cannot occur until the third residue of this peptide, where the backbone amide of E3 could form a hydrogen bond with the carbonyl group of the *N*-acetyl group for an α-helix, or with the carbonyl group of E1 for a 3_{10}-helix.

Lactam Ring. NOE connectivities confirm the presence of lactam rings bridging the γ-carbonyls of E3 and E10 and the ϵ-amides of K7 and K14, respectively. Strong E3γ2/K7ϵNH and E10γ2/K14ϵNH as well as weaker E3β2/K7ϵNH and E10β2/K14ϵNH NOEs are observed in the JR-NOESY spectrum at 5.0 °C and the ROESY spectrum at 25.0 °C.

Proton chemical shifts measured at both 5.0 °C and 25.0 °C also provide evidence for the presence of the lactam rings. From Table 3, it can be seen that the proton chemical shifts of the side chain protons of E3, E10, K7, and K14 are anomalously shifted from those values observed for the side chain protons of E1, E8, K6, and K13, residues not involved in the formation of the lactam bridge. The chemical shift values measured at 5.0 °C (Table 3A) show that the γ protons of E3 and E10 are downfield shifted by >0.15 ppm from those values observed for the γ protons of E1 and E8, and the chemical shift dispersion between the β protons of E3 and E10 is much larger (>0.4 ppm) than that observed between the β protons of E1 and E8 (<0.1 ppm), suggesting that the chemical environment of the β protons of E3 and E10 becomes much more unequivalent upon formation of the lactam ring. It can also be seen that the chemical shift dispersion between the γ protons and the ϵ protons of K7 and K14 is >0.2 ppm for the γ protons and >0.7 ppm for the ϵ protons, whereas the γ and ϵ protons of K6 and K13 are chemically shift degenerate. This suggests that the chemical environment of the γ protons and the ϵ protons of K7 and K14 also becomes much more unequivalent upon formation of the lactam ring. In addition, the δ and ϵNH protons of K7 and K14 are downfield shifted by >0.15 ppm for the δ protons and downfield shifted by >0.3 ppm for ϵNH protons from those values observed for the δ and ϵNH protons of K6 and K13. Indeed, the ϵNH resonances of K6 and K13 are broadened at 5 °C and are not even visible in the spectrum at 25 °C due to very rapid chemical exchange; however, the ϵNH resonances of K7 and K14 not only are visible at 25 °C but also are very sharp and intense, showing minimal chemical exchange owing to their involvement in the lactam ring.

DISCUSSION

The effect of incorporating two Glu-Lys $i,i+4$ lactam bridges into small amphipathic peptides based on a 3,4 repeat is profound. The linear, non-lactam-bridged peptides, which have the same sequence as the lactam-bridged peptides, were considerably less helical than their lactam homologs, even though the potential for i to $i+4$ salt bridges exists in these peptides. In general, the amount of helicity induced by the incorporation of lactam bridges (Table 1, linear−lactam) is similar in magnitude to that seen with the linear peptides in 50% TFE (Table 1, linear−50% TFE).

In addition to stabilizing helical structure, lactam bridges appear to enhance peptide−peptide interactions. For peptide 2EKI, SEC indicates that the peptide associates as a dimer. Previously it has been shown that 23 residues or 6 complete turns are required for a synthetic sequence based on the 3,4 repeat (EIEALKA) to associate as a dimer (Su et al., 1994). This repeating heptad differs from the heptad of 2EKI by changing Lys at *f* positions to an Ala. Since these two heptad repeats are comparable, it suggests that lactam-bridged peptides can associate as dimers at a peptide length as low as 14 residues. While the concentration dependency of 2EKV indicates that interchain interactions are important in stabilizing helical structure, the corresponding dimer peak was not observed during SEC. The lack of a plateau in the plot of molar ellipticity at 222 nm versus peptide concentration for peptide 2EKV indicates that these quaternary interactions are less effective in stabilizing helical structure compared to peptide 2EKI. The enhancement of interchain interactions for the lactam-bridged peptides may result from the N- and C-termini of the lactam-bridged peptides being locked into an α-helical conformation. Due to an absence of fraying, the nonpolar face remains consistently helical and maximizes the hydrophobic interactions required for dimerization. The linear peptides would be expected to have ends which are frayed and deviate from the helical conformation (Dyson & Wright, 1991; O'Shea et al., 1991; Zhou et al., 1992a).

By decreasing the hydrophobicity further through substitution of Val by Ala, a more helical peptide is generated. The lack of a dependence of the molar ellipticity at 222 nm on peptide concentration indicates that peptide−peptide interactions do not stabilize the helical structure and suggests the peptide is monomeric. This was further demonstrated by SEC. In addition, ^{1}H NMR spectra run at 2 mM and 200 μM (data not shown) indicated there was no change in line width, lending further evidence that this peptide exists as a monomeric species. The switch from a dimeric entity (2EKI) to a fully helical monomer (2EKA) suggests that there is a critical level of hydrophobicity required for dimerization.

It has been suggested that short alanine-based peptides may exist predominantly in the 3_{10} conformation instead of the α-helix (Miick et al., 1992; Fiori et al., 1993). From our CD and NMR results, this does not appear to be the case. Theoretically determined CD profiles for the α-helix and 3_{10}-helix suggest that while both types of helices should have similarly intense bands at 222 nm, the 3_{10}-helix should have a much more intense band at 208 nm than at 222 nm (Manning & Woody, 1991). As shown in Figure 1, the CD spectra of 2EKA are consistent with the α-helical conformation.

The NMR data are consistent with peptide 2EKA adopting a helical conformation. First, all αCH protons are upfield shifted relative to random-coil values (Wishart et al., 1991), with the greatest upfield shifts observed for residues constrained within the lactam bridge. Also, $^3J_{NH\alpha CH}$ coupling constants extracted from the DQF COSY spectrum, which vary from 4 to 6 Hz, suggest that 2EKA exists in a helical conformation. The temperature dependence of the amide chemical shifts indicates values of $-\Delta\delta/\Delta T \leq 4$ ppb for residues Glu3 to Lys14, which is consistent with these amides participating in C═O···NH hydrogen bonds. The larger values observed for Glu1 and Ala2 are consistent with the fact that these residues would lack hydrogen bonding partners if 2EKA adopts a helical conformation. NOE connectivities predictive of a helical conformation include $d_{NN}(i,i+1)$, $d_{NN}(i,i+2)$, $d_{\alpha N}(i,i+3)$, and $d_{\alpha\beta}(i,i+3)$ connectivities, which are found in the NOESY spectrum of peptide 2EKA. In addition, the existence of strong sequential $d_{NN}(i,i+1)$ connectivities followed by the diminution of the intensity of $d_{\alpha N}(i,i+1)$ NOEs is a further indication that 2EKA adopts an α-helical confirmation (Dyson & Wright, 1991; Zhou et al., 1992b). The existence of $d_{\alpha N}(i,i+2)$ connectivities may indicate that a portion of the C-terminus may populate a 3_{10}-helix. Alternatively, modeling studies suggest that the amide hydrogen of the carboxamide functionality can hydrogen bond to the carbonyl oxygen of Ala11. This hydrogen

bonding tends to shorten the pitch of this area of the helix, resulting in a conformation that resembles a type II β-turn which might be the source of these NOEs (Pierre Lavigne, personal communication).

The thermal denaturation profiles of all lactam-bridged peptides were found to be reversible as indicated by recovery of the CD spectra upon cooling. All the thermal melting curves demonstrated the existence of an isodichroic point at 204 nm, indicating the transitions proceed by a two-state mechanism. At higher temperatures, the CD spectra resemble the superposition of helical and random-coil conformations. Such spectra are most likely due to residues constrained within the lactam bridges remaining helical while those outside are free to populate random-like conformations.

For the monomeric peptide, the high helical content is quite remarkable when compared to other short peptides. Previously studied alanine-based peptides attain high helical content at 0 °C and low ionic strength buffers but quickly denature as the temperature is raised (Marqusee & Baldwin, 1987; Marqusee et al., 1989). Using a similar sequence, Ghadiri and Choi (1990) were able to design a transition metal ion stabilized helix that was 80% helical at 21 °C. However, the calculated helicity of peptide 2EKA based on the $[\theta]_{222}$ values suggests this peptide is essentially 100% at 20 °C. Moreover, the pattern of NOEs observed at 5 °C is identical to those observed at 25 °C, further demonstrating the helical stability of the peptide.

This study demonstrates that Glu to Lys *i* to *i*+4 lactam bridges can be effectively utilized in designing highly stable α-helical peptides which are both monomeric and dimeric. CD and 2D NMR experiments show that the monomeric peptide is highly helical through its entire length. Moreover, residues found within the lactam bridge (EAL) are most strongly constrained into a helical conformation, indicating the efficacy of these bridges in stabilizing and inducing helical structure. As a consequence of placing lactam bridges near the termini of the peptide, they may enhance dimerization of small peptides by negating end effects and presenting a nonpolar face which maximizes hydrophobic interactions. This study also suggests there is a critical level of hydrophobicity required for dimerization to take place. The above system may serve as a model in the study of protein folding and determining α-helical propensities of amino acids. This model may also be applicable to study protein−protein interactions and may prove useful in the *de novo* design of helical peptides with enhanced biological activities.

ACKNOWLEDGMENT

We thank Bob Luty for his skilled technical assistance in performing circular dichroism measurements and Mrs. Terri Stelfox for amino acid analysis.

REFERENCES

Bax, A., & Davis, D. G. (1985) *J. Magn. Reson. 65*, 355−360.
Brown, J. E., & Klee, W. A. (1971) *Biochemistry 10*, 470−476.
Chen, Y.-H., Yang, J. T., & Chau, K. H. (1974) *Biochemistry 13*, 3350−3359.
Dyson, H. J., & Wright, P. E. (1991) *Annu. Rev. Biophys. Chem. 20*, 519−538.
Felix, A. M., Heimer, E. P., Wang, C.-T., Lambros, T. J., Fournier, A., Mowles, T. F., Maines, S., Campbell, R. M., Wegrzynski, B. B., Toome, V., Fry, D., & Madison, V. S. (1988) *Int. J. Pept. Protein Res. 32*, 441−454.
Fiori, W. R., Miick, S. M., & Millhauser, G. L. (1993) *Biochemistry 32*, 11957−11962.
Gagné, S. M., Tsuda, S., Li, M. X., Chandra, M., Smillie, L. B., & Sykes, B. D. (1994) *Protein Sci. 3*, 1961−1974.
Ghadiri, M. R., & Choi, C. (1990) *J. Am. Chem. Soc. 112*, 1630−1632.
Goodman, M., & Listowsky, I. (1962) *J. Am. Chem. Soc. 84*, 3370−3371.
Goodman, M., Naider, F., & Toniolo, C. (1971) *Biopolymers 10*, 1719−1730.
Guéron, M., Plateau, P., Kettani, A., & Decorps, M. (1992) *J. Magn. Reson. 96*, 541−550.
Hodges, R. S., Zhou, N. E., Kay, C. M., & Semchuk, P. D. (1990) *Pept. Res. 3*, 123−137.
Houston, M. E., Jr., Gannon, C. L., Kay, C. M., & Hodges, R. S. (1995) *J. Pept. Sci. 1*, 274−282.
Jackson, D. Y., King, D. S., Chmielewski, J., Singh, S., & Schultz, P. G. (1991) *J. Am. Chem. Soc. 113*, 9391−9392.
Jeener, J., Meier, B. H., Bachmann, P., & Ernst, R. R. (1979) *J. Chem. Phys. 71*, 4546−4553.
Kemp, D. S., Boyd, J. G., & Muendel, C. C. (1991) *Nature 352*, 451−454.
Kessler, H., Griesinger, C., Kerssebaum, R., Wagner, K., & Ernst, R. R. (1987) *J. Am. Chem. Soc. 109*, 607−609.
Lau, S. Y. M., Taneja, A. K., & Hodges, R. S. (1984) *J. Chromatogr. 317*, 129−140.
Lehrman, S. R., Tuls, J. L., & Lund, M. (1990) *Biochemistry 29*, 5590−5596.
Macura, S., & Ernst, R. R. (1980) *Mol. Phys. 41*, 95−117.
Madison, V. S., Fry, D. C., Greeley, D. N., Toome, V., Wegrzynski, B. B., Heimer, E. P., & Felix, A. M. (1990) in *Peptides: Chemistry, Structure and Biology, Proceedings of the Eleventh American Peptide Symposium* (Rivier, J. E., & Marshall, G. R., Eds.) pp 575−577, ESCOM Science Publishers, Leiden, The Netherlands.
Manning, M. C., & Woody, R. W. (1991) *Biopolymers 31*, 569−586.
Marqusee S., & Baldwin, R. L. (1987) *Proc. Natl. Acad. Sci. U.S.A. 84*, 8898−8902.
Marqusee, S., Robbins, V. H., & Baldwin, R. L. (1989) *Proc. Natl. Acad. Sci. U.S.A. 86*, 52865290.
Miick, S. M., Martinez, G. V., Fiori, W. R., Todd, A. P., & Millhauser, G. L. (1992) *Nature 359*, 653−655.
Monera, O. D., Sereda, T. J., Zhou, N. E., Kay, C. M., & Hodges, R. S. (1995) *J. Pept. Sci. 1*, 319−329.
Osapay, G., & Taylor, J. W. (1990) *J. Am. Chem. Soc. 112*, 6046−6051.
O'Shea, E. K., Klemm, J. D., Kim, P. S., & Alber, T. (1991) *Science 254*, 539−544.
Padmanabhan, S., Marqusee, S., Ridgeway, T., Laue, T. M., & Baldwin, R. L. (1990) *Nature 344*, 268−270.
Pardi, A., Billeter, M., & Wüthrich, K. (1984) *J. Mol. Biol. 180*, 741−751.
Piatini, U., Sorenson, O. W., & Ernst, R. R. (1982) *J. Am. Chem. Soc. 104*, 6800−6801.
Plateau, P., & Guéron, M. (1982) *J. Am. Chem. Soc. 104*, 7310−7311.
Rance, M., Sorenson, O. W., Bodenhausen, G., Wagner, G., Ernst, R. R., & Wüthrich, K. (1983) *Biochem. Biophys. Res. Commun. 117*, 479−485.
Rose, G. D., Gierasch, L. M., & Smith, J. A. (1985) *Adv. Protein Chem. 37*, 1−107.
Scholtz, J. M., & Baldwin, R. L. (1992) *Annu. Rev. Biophys. Biomol. Struct. 21*, 95−118.
Shoemaker, K. R., Kim, P. S., Brems, D. N., Marqusee, S., York, E. J., Chaiken, I. M., Stewart, J. M., & Baldwin, R. L. (1985) *Proc. Natl. Acad. Sci. U.S.A. 82*, 2349−2353.
Shoemaker, K. R., Kim, P. S., York, E. J., Stewart, J. M., & Baldwin, R. L (1987) *Nature 326*, 563−567.
Sönnichsen, F. D., Van Eyk, J. E., Hodges, R. S., & Sykes, B. D. (1992) *Biochemistry 31*, 8790−8798.
States, D. J., Haberkorn, R. A., & Ruben, D. J. (1982) *J. Magn. Reson. 48*, 286−292.
Su, J. Y., Hodges, R. S., & Kay, C. M. (1994) *Biochemistry 33*, 15501−15510.
Wagner, G., Neuhaus, D., Wîrgîtter, E., Vasák, M., Kägi, J. H. R., & Wüthrich, K. (1986) *J. Mol. Biol. 187*, 131−135.

Wishart, D. S., Sykes, B. D., & Richards, F. M. (1991) *J. Mol. Biol. 222*, 311−333.
Wüthrich, K. (1986) in *NMR of Proteins and Nucleic Acids*, John Wiley and Sons, New York.
Wüthrich, K., Billeter, M., & Braun, W. (1984) *J. Mol. Biol. 180*, 715−740.
Zhou, N. E., Kay, C. M., & Hodges, R. S. (1992a) *J. Biol. Chem. 267*, 2664−2670.
Zhou, N. E., Zhu, B.-Y., Sykes, B. D., & Hodges, R. S. (1992b) *J. Am. Chem. Soc. 114*, 4320−4326.
Zhou, N. E., Zhu, B.-Y., Kay, C. M., & Hodges, R. S. (1993a) in *Peptides: Biology and Chemistry, Proceeding of the 1992 Chinese Peptide Symposium* (Du, Y.-C., Tam, J. P., & Zhang, Y.-S., Eds.) pp 217−220, ESCOM Science Publishers, Leiden, The Netherlands.
Zhou, N. E., Kay, C. M., Sykes, B. D., & Hodges, R. S. (1993b) *Biochemistry 32*, 6190−6197.
Zhou, N. E., Monera, O. D., Kay, C. M., & Hodges, R. S. (1994) *Protein Pept. Lett. 1*, 114−119.
Zhu, B.-Y., Zhou, N. E., Kay, C. M., & Hodges, R. S. (1993) *Protein Sci. 2*, 383−394.

BI952757M